Available online at www.sciencedirect.com
SCIENCE DIRECT
Polymer 46 (2005) 3942–3951
polymer
www.elsevier.com/locate/polymer

Effects of neutral solvent addition on the body-centered cubic spheres of block copolymers

Yung Chang[a], Hsiao-Yang Hsueh[b], Wen-Chang Chen[a,b], Ching-I Huang[b,*]

[a]*Department of Chemical Engineering, National Taiwan University, Taipei 106, Taiwan, ROC*
[b]*Institute of Polymer Science and Engineering, National Taiwan University, Taipei 106, Taiwan, ROC*

Received 15 October 2004; received in revised form 21 February 2005; accepted 27 February 2005
Available online 7 April 2005

Abstract

We employ self-consistent mean-field (SCMF) theory in studying the body-centered cubic (bcc) spheres of block copolymers in the presence of a neutral solvent. First we examine the accuracy of the dilution approximation then analyze the dependence of the bcc structural sizes with copolymer volume fraction ϕ, the interaction parameter χ_{AB}, and degree of copolymerization N. Our results reveal that both distribution of each component and the micro-structural length scales are greatly influenced by each parameter ϕ, χ_{AB}, and N. As expected, with decreasing ϕ, more solvent distributes non-uniformally in the segregated domains, therefore deviation from the dilution approximation increases. This also suggests that when the effective segregation parameter $\phi\chi_{AB}N$ is fixed, a larger deviation is expected as $\chi_{AB}N$ increases (i.e. ϕ decreases). Although when both $\chi_{AB}N$ and ϕ are fixed, decreasing N (i.e. increasing χ_{AB}) enlarges the deviation from the dilution approximation. Furthermore, this solvent non-uniformity behavior is so significant that it even affects the dependence of the domain spacing L^* and the matrix length Λ^* with respect to $(\chi_{AB})_{eff}N=\phi\chi_{AB}N$ near the ODT. When the systems are in molten state and/or in the concentrated regime, both L^* and Λ^* exhibit a sharp increase behavior as ODT is approached, due to many of the minority blocks being pulled from the spherical domains and swelling the matrix. With increasing solvent amount and/or $\chi_{AB}N$, we observe that the increase of the degree for the minority blocks pulled from the spheres into the matrix near the ODT is not as significant as that in the melt. As such, the sharp increase behavior in L^* as well as Λ^* near the ODT smoothens and even disappears.

Keywords: Self-consistent mean-field theory; Block copolymer solutions; Dilution approximation

1. Introduction

Block copolymers continue to be an attractive area of research due to their numerous potential applications with characteristic domain dimensions in the range of 1–100 nm by self-organization [1–3]. One of the major methods in controlling the length scale of microstructures is by diluting a block copolymer with solvent. Adding solvent S into an A/B diblock copolymer, both the phase behavior and the micro-domain length control become more complicated as they involve the effects of copolymer composition f, degree of copolymerization N, copolymer volume fraction ϕ, and three independent interaction parameters, χ_{AB}, χ_{AS}, and χ_{BS}.

In the neutral (i.e. $\chi_{AS}=\chi_{BS}$), there has been a great deal of theoretical [4–13] and experimental [14–25] studies on the resulting equilibrium phase behavior and the scaling behavior of micro-domain spacing. Provided the concentrated regime and the solvent quality are good, the solvent is distributed almost uniformly between the segregated micro-domains. Consequently, the solution behaves as a neat copolymer with the effective A/B interaction parameter $(\chi_{AB})_{eff}$ simply given as $\phi\chi_{AB}$, which is named 'dilution approximation' [4]. Previous self-consistent mean-field (SCMF) calculations have shown that the equilibrium solution phase maps are almost identical to the melt phase map by replacing $\chi_{AB}N$ with $\phi\chi_{AB}N$ [5,8,9,11]. To explain further, the order-order transitions (OOTs) and order-disorder transition (ODT) for concentrated solutions follow $(\phi\chi_{AB}N)_{ODT,OOT}=F(f)$, as given in the melts. In the semi-dilute regime due to the chain swelling effects, both Olvera

* Corresponding author. Tel.: +886 2 33665886; fax: +886 2 33665237.
E-mail address: chingih@ntu.edu.tw (C.-I. Huang).

0032-3861/$ - see front matter © 2005 Elsevier Ltd. All rights reserved.
doi:10.1016/j.polymer.2005.02.103

de la Cruz [7] and Fredrickson and Leibler [6] predicted $(\phi^{1.59}\chi_{AB}N)_{ODT}=F(f)$. Although experiments have shown that the dilution approximation fails to describe the ODT even for concentrated block copolymer solutions due to the fluctuation effects [17,23–25], it is still successful in predicting the OOTs [23–25] and micro-domain spacings [14,15,23–25].

Whitmore and Noolandi [8] examined the lamellar structure for copolymers in the presence of a neutral good solvent by SCMF theory. They found that with a small amount of solvent accumulation at the interface the dependence of the lamellar domain spacing L with χ_{AB}, N, and ϕ is still approximated by

$$L \sim (\chi_{AB})^p N^q \phi^r \tag{1}$$

with $p\cong 0.33$, $q\cong 0.8$, and $r\cong 0.4$ being in the weak segregation regime, and $p\cong 0.2$, $q\cong 0.67$, and $r\cong 0.22$ in the strong segregation regime. Furthermore, Vavasour and Whitmore [10] showed that the micro-domain spacing for lamellar, cylindrical, and spherical structures obeys the dilution approximation, i.e. the spacing L^*, which is in terms of the mean-squared end-to-end distance ($\sqrt{N}b$), scales approximately as

$$L^* \sim (\phi\chi_{AB}N)^{\alpha} \tag{2}$$

with α equal to 0.2 in the strong segregation regime. This is independent of morphology, and increases to a value equal to 0.5 for lamellar phase and 0.4 for cylindrical phase as the ODT is approached. α for the spherical phase is close to 0.2 in the whole segregation regime. These domain spacing scaling predictions have been observed in agreement with experiments [14,15, 23–25]. For example, Lodge et al. examined a series of poly (styrene-block-isoprene) diblock copolymers in the presence of a neutral solvent dioctyl phthalate [23–25]. They found that the characteristic domain spacing scales as $\phi^{0.33}$ and $\chi^{0.25}$, which is independent of morphology. Hashimoto et al. reported the lamellar spacing as $L\sim(\phi\chi_{AB})^{1/3}$ [14,15]. However, with the effects of solvent accumulation at the interface, the question still remains of just how good the dilution approximation is by varying χ_{AB}, N, and ϕ. Also the detailed analysis for the length scales of each segregated domain, such as the A-rich and B-rich phases, as well as the interfacial width as a function of χ_{AB}, N, and ϕ remains unexplored. Although Naughton and Matsen [13] have employed SCMF theory to examine the accuracy of the dilution approximation as a function of solvent quality, size, and selectivity, they did not analyze the solvent effects on the behavior for each segregated domain spacing.

In this paper we address the issue on the body-centered cubic (bcc) spheres of block copolymers in a neutral good solvent using SCMF theory. First, we examine the effects of χ_{AB}, N, and ϕ on the resulting volume fraction profiles of each component. We then analyze how the distribution of each component affects the related micro-structural domain length scales, such as the domain lattice spacing L^*, the spherical diameter D^*, the interfacial width w^*, and the matrix length $\Lambda^*(=L^*-D^*-w^*)$. It is worth noting that as the ODT is approached, both L^* and Λ^* for the solutions in the bcc phase exhibit a unique behavior, which has not been observed elsewhere.

2. Theory

We employ self-consistent mean-field (SCMF) theory to analyze the structural length scales in the ordered body-centered cubic (bcc) spheres of block copolymer solutions, by using a previously established formalism [11]. As the block copolymer morphologies are periodic, it is most efficient to perform the SCMF calculations using the Fourier-space algorithm. That is, any given function, $g(r)$ is expressed in terms of the corresponding amplitudes, g_j, with respect to a series of orthonormal basis function $f_j(r)$, $g(r)=\sum_j g_j f_j(r)$. The basis functions reflect the symmetry of the ordered phase being considered, and are selected to be eigenfunctions of the Laplacian operator

$$\nabla^2 f_j(r) = -\lambda_j L^{-2} f_j(r) \tag{3}$$

where L is the lattice spacing for the ordered phase. The basis functions are ordered starting with $f_1(r)=1$ such that λ_j is an increasing series. For both bcc and fcc phases $f_j(r)=C_j\cos(2\pi hx/L)\cos(2\pi ky/L)\cos(2\pi lz/L)$, where x, y, z are the coordinates and h, k, l are all integers. In particular, for bcc spheres $h+k+l$ has to be even, and h, k, and l are all even or odd for fcc. The coefficients C_j are determined by satisfying $1/L\int f_j^2(r)\mathrm{d}r=1$.

We consider a monodisperse AB diblock copolymer in the presence of a solvent with average volume fractions ϕ and $1-\phi$, respectively, The degree of copolymerization is N and A-monomer fraction in the copolymer is f. We assume that the system is incompressible both locally and globally, and each monomer type has the same statistical segment length b. The local interaction between each pair of monomers I and J, is quantified by the Flory–Huggins interaction parameter χ_{IJ}. Each copolymer chain is parameterized by a variable s that increases continuously from 0 to 1 along its length. We assume that the A-block starts from $s=0$ and terminates at $s=f$ which is the A–B junction point. In order to determine the concentration profiles as well as the free energy in the equilibrium state, it is necessary to solve two end-segment copolymer distribution functions, $q_C(r,s)$ and $q_C^+(r,s)$. These are found by integrating all possible configurations subject to the fields $\omega_A(r)$ and $\omega_B(r)$ for chain segments running from $s=0$ to f and from $s=f$ to 1, respectively, and the solvent distribution function $q_S(r,s)$

subject to the field $\omega_S(r)$. The distribution function $q_C(r,s)$ satisfies the modified diffusion equation,

$$\frac{\partial q_C}{\partial s} = \begin{cases} \frac{1}{6}Nb^2\nabla^2 q_C - \omega_A q_C & \text{if } s<f \\ \frac{1}{6}Nb^2\nabla^2 q_C - \omega_B q_C & \text{if } s>f \end{cases} \quad (4)$$

and the initial condition is, $q_C(r,0)=1$. The equation for $q_C^+(r,s)$ is similar except that the right-hand side of Eq. (4) is multiplied by -1, and the initial condition is $q_C^+(r,1)=1$. Since there is no chain connectivity in the solvent distribution function $q_S(r,s)$ becomes

$$\frac{\partial q_S}{\partial s} = -\omega_S q_S \quad (5)$$

When the amplitudes corresponding to the basis functions are utilized, the modified diffusion Eqs. (4) and (5) in terms of $q_{C,i}(s)$, $q_{C,i}^+(s)$, and $q_{S,i}(s)$, become

$$\frac{\partial q_{C,i}}{\partial s} = \begin{cases} \sum_j A_{ij} q_{C,j} & \text{if } s<f \\ \sum_j B_{ij} q_{C,j} & \text{if } s>f \end{cases} \quad i=1,2,3,\ldots \quad (6)$$

$$\frac{\partial q_{S,i}}{\partial s} = \sum_j C_{ij} q_{S,j} \quad i=1,2,3,\ldots \quad (7)$$

The equation for $q_{C,i}^+$ is similar except that the right-hand side of Eq. (6) is multiplied by -1. The initial conditions are $q_{C,i}(s=0)=\delta_{i1}$, $q_{C,i}^+(s=1)=\delta_{i1}$, and $q_{S,i}(s=0)=\delta_{i1}$. The matrices A_{ij}, B_{ij}, and C_{ij} are given by

$$A_{ij} = -\frac{Nb^2}{6L^2}\lambda_i\delta_{ij} - \sum_k \omega_{A,k}\Gamma_{ijk}$$

$$B_{ij} = -\frac{Nb^2}{6L^2}\lambda_i\delta_{ij} - \sum_k \omega_{B,k}\Gamma_{ijk} \quad (8)$$

$$C_{ij} = -\sum_k \omega_{S,k}\Gamma_{ijk}$$

$\Gamma_{ijk} = V^{-1}\int f_i(r)f_j(r)f_k(r)\mathrm{d}r$. $\omega_{A,k}$, $\omega_{B,k}$, and $\omega_{S,k}$ are the corresponding amplitudes with respect to the kth basis function for fields ω_A, ω_B, and ω_S, respectively. Based on the minimization of free energy to attain thermodynamic equilibrium for a periodic ordered phase, the amplitudes of the fields have to satisfy

$$\begin{aligned} \omega_{A,i} - \omega_{S,i} &= \chi_{AB}N\phi_{B,i} + \chi_{AS}N\phi_{S,i} - \chi_{AS}N\phi_{A,i} \\ &\quad - \chi_{BS}N\phi_{B,i} \\ \omega_{B,i} - \omega_{S,i} &= \chi_{AB}N\phi_{A,i} + \chi_{BS}N\phi_{S,i} - \chi_{AS}N\phi_{A,i} \\ &\quad - \chi_{BS}N\phi_{B,i} \\ \phi_{A,i} + \phi_{B,i} + \phi_{S,i} &= \delta_{i1} \end{aligned} \quad (9)$$

where the amplitudes of the concentrations of A, B and S, respectively, $\phi_{A,j}$, $\phi_{B,j}$, and $\phi_{S,j}$ are expressed in terms of the distribution functions

$$\phi_{A,i} = \frac{\phi}{q_{C,1}(1)}\sum_{j,k}\Gamma_{ijk}\int_0^f \mathrm{d}s q_{C,j}(s)q_{C,k}^+(s)$$

$$\phi_{B,i} = \frac{\phi}{q_{C,1}(1)}\sum_{j,k}\Gamma_{ijk}\int_f^1 \mathrm{d}s q_{C,j}(s)q_{C,k}^+(s) \quad (10)$$

$$\phi_{S,i} = q_{S,i}(1/N)$$

Once the above amplitudes are determined and the self-consistent equations for the fields are satisfied, the free energy per molecule F is given by

$$\begin{aligned} \frac{F}{k_BT} &= -\phi\ln\left[\frac{q_{C,1}(1)}{\phi}\right] - (1-\phi)N\ln\left[\frac{q_{C,1}(1/N)}{1-\phi}\right] \\ &\quad - \sum_i(\omega_{A,i}\phi_{A,i} + \omega_{B,i}\phi_{B,i} + \omega_{S,i}\phi_{S,i}) \\ &\quad + \sum_i(\chi_{AB}N\phi_{A,i}\phi_{B,i} + \chi_{AS}N\phi_{A,i}\phi_{S,i} \\ &\quad + \chi_{BS}N\phi_{B,i}\phi_{S,i}) \end{aligned} \quad (11)$$

which is reduced to the Flory–Huggins mean-field free energy functional in the disordered state. For a periodic ordered phase, the free energy has to be minimized with respect to the lattice spacing L. As our major study is to examine the structural length scales in the bcc array, we choose the particular parameters in that bcc is the most stable phase. Once the lattice spacing L is obtained, we determine the spherical diameter D, the interfacial width w, and the matrix length Λ as follows. For example, when a neutral solvent ($\chi_{AS}=\chi_{BS}=0.4$) is added into a block copolymer with $f=0.16$, $N=300$, $\phi=0.8$, and $\chi_{AB}N=41.4$, the ordered bcc array of A-rich spheres (S_A^{BCC}) is the most stable phase. Fig. 1(a) and (b) display the corresponding contour plots of A volume fraction profiles at X–Y plane in the z-axis of $z/L=0$ and $z/L=0.5$, respectively. As can be clearly seen, the A-block forms spheres in the bcc array. Fig. 1(c) shows the typical volume fraction profiles ϕ_A, ϕ_B and ϕ_S at $y/L=z/L=0.5$, from which the inflection points with respect to ϕ_A, ϕ_B and ϕ_S; i.e. $\mathrm{d}^2\phi_I/\mathrm{d}x^2=0$ (I=A, B, S) are determined. Note that these inflection points are identical. As such, both values of the spherical diameter D and the interfacial width w are determined, as shown in Fig. 1(c). The matrix domain length Λ is defined as $L-D-w$.

Once the micro-domains are divided into distinct spherical, interfacial, and matrix regimes, the volume fractions of each component A, B and S, which are partitioned into spheres, interface, and matrix, $\phi_J^{(S)}$, $\phi_J^{(W)}$, and $\phi_J^{(M)}$, respectively, J=A, B, S, are calculated by the following equations:

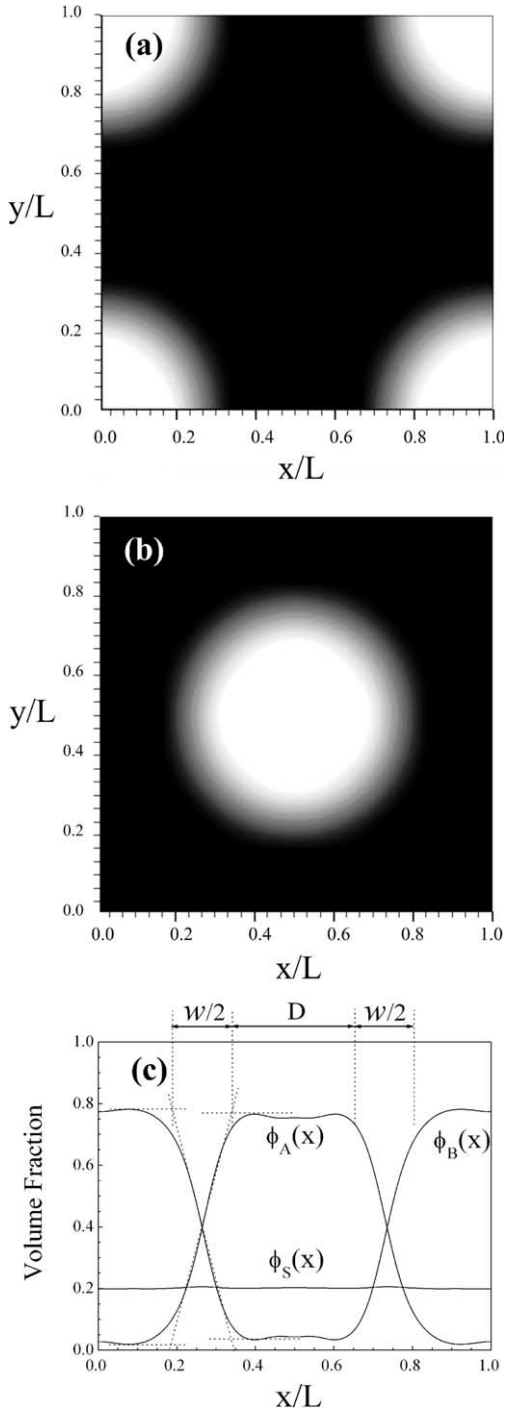

Fig. 1. Contour plots of A volume fraction profiles at X–Y plane in the z-axis of (a) $z/L=0$ and (b) $z/L=0.5$, respectively, and (c) volume fraction profiles of ϕ_A, ϕ_B, and ϕ_S at $y/L=z/L=0.5$ for block copolymer solutions in the S_A^{BCC} phase with $f=0.16$, $N=300$, $\phi=0.8$, $\chi_{AB}=0.138$, and $\chi_{AS}=\chi_{BS}=0.4$.

$$\phi_J^{(S)} = \frac{1}{L^3}\int_{V_S} \phi_J(r)\mathrm{d}^3 r$$

$$\phi_J^{(W)} = \frac{1}{L^3}\int_{V_W} \phi_J(r)\mathrm{d}^3 r \quad J = A, B, S \tag{12}$$

$$\phi_J^{(M)} = \frac{1}{L^3}\int_{V_M} \phi_J(r)\mathrm{d}^3 r$$

where

$$V_S = 2(4\pi/3)(D/2)^3$$

$$V_W = 2\frac{4\pi}{3}\left[\left(\frac{D}{2}+\frac{w}{2}\right)^3 - \left(\frac{D}{2}\right)^3\right]$$

and $V_M = L^3 - V_S - V_W$. It is evident that the sum of $\phi_J^{(S)}$, $\phi_J^{(W)}$, and $\phi_J^{(M)}$ is equal to the average volume fraction of component $J(\bar{\phi}_J)$. Therefore, the relative volume fraction of component J into each regime is equal to

$$\tilde{\phi}_J^{(S)} = \frac{\phi_J^{(S)}}{(\phi_J^{(S)}+\phi_J^{(W)}+\phi_J^{(M)})} = \frac{\phi_J^{(S)}}{\bar{\phi}_J}$$

$$\tilde{\phi}_J^{(W)} = \frac{\phi_J^{(W)}}{(\phi_J^{(S)}+\phi_J^{(W)}+\phi_J^{(M)})} = \frac{\phi_J^{(W)}}{\bar{\phi}_J} \quad J = A, B, S \tag{13}$$

$$\tilde{\phi}_J^{(M)} = \frac{\phi_J^{(M)}}{(\phi_J^{(S)}+\phi_J^{(W)}+\phi_J^{(M)})} = \frac{\phi_J^{(M)}}{\bar{\phi}_J}$$

Note that in Section 3 we use the dimensionless length parameters L^*, D^*, w^* and Λ^*, which are in terms of the mean-squared end-to-end distance of copolymer chains ($\sqrt{N}b$), i.e. $L^* = L/\sqrt{N}b$ and similar to D^*, w^* and Λ^*.

3. Results and discussion

To study the effects of neutral solvent addition on bcc spheres of block copolymers, we choose a model system with $f=0.16$ and $\chi_{AS}=\chi_{BS}=0.4$, and vary the values of χ_{AB}, N, and ϕ ranging from

$$0.06 \le \chi_{AB} \le 0.45$$

$$150 \le N \le 1000$$

$$0.2 \le \phi \le 1.0$$

Typical phase maps in terms of $\chi_{AB}N$ and ϕ are shown in Fig. 2, where N is equal to 150. In order to examine the possibility of dilution approximation holding for both order-order and order-disorder transitions, we also plot the calculated transition values directly from the dilution approximation as the dotted curves in Fig. 2. Similar to melts [26], the trends in phase transitions from hexagonally close-packed cylinders of A (C_A)→bcc spheres of A (S_A^{BCC})→fcc spheres of A (S_A^{FCC})→disordered phase (D) with decreasing $\chi_{AB}N$ are preserved. It is clear that the boundaries between S_A^{FCC}/D and S_A^{BCC}/S_A^{FCC} deviate more from the dilution approximation with ϕ decreasing. We also observe that this deviation degree decreases with N increasing. These results concur with those of Whitmore

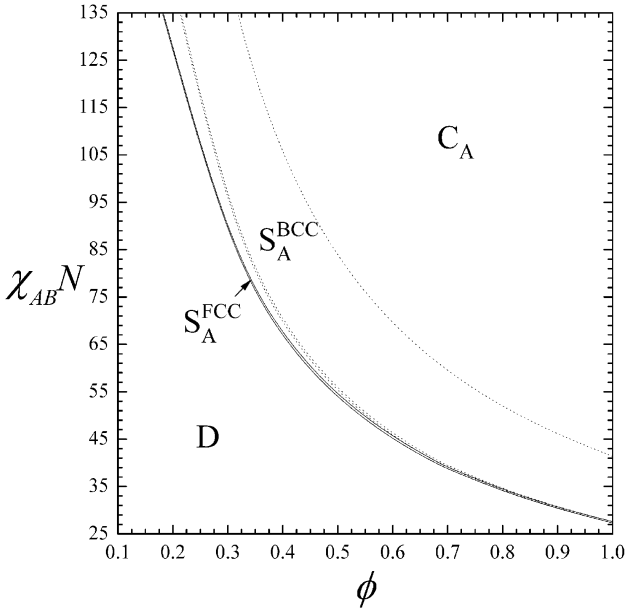

Fig. 2. Phase diagram for a diblock copolymer with $f=0.16$ and $N=150$ in a neutral solvent ($\chi_{AS}=\chi_{BS}=0.4$) as a function of ϕ and $\chi_{AB}N$. The dotted curves correspond to the transition curves simply from the dilution approximation.

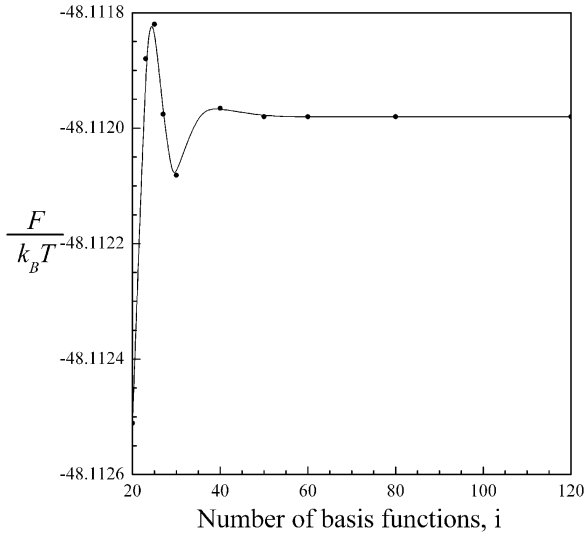

Fig. 3. Free energy per molecule F in Eq. (11) as a function of number of the basis functions for a copolymer with $f=0.16$ in a neutral solvent with $\chi_{AS}=\chi_{BS}=0.4$ when $\phi\chi_{AB}N=40$ ($\phi=0.2963$, $\chi_{AB}=0.45$ and $N=300$).

and Vavasour [9]. It should be noted that although SCMF theory predicts a very narrow window of S_A^{FCC} phase near the ODT, the most probable order for the minority A spheres is bcc. In addition, there exists to our knowledge, no experimental evidence for fcc spheres in the neutral solvent case. Therefore, we then focus on the analysis of the micro-structural lengths for S_A^{BCC} phase. In particular, the effective segregation regime for our model system with $f=0.16$ is $27.6\leq(\chi_{AB})_{eff}N=\phi\chi_{AB}N\leq41.4$ in order to assure that bcc is the stable phase. Note that the number of basis functions in our computations is 60, since the free energy per molecule F in Eq. (11) obtained for 60 basis functions already reaches the equilibrium value. For example, Fig. 3 plots F versus number of basis functions for a copolymer with $f=0.16$ in a neutral solvent with $\chi_{AS}=\chi_{BS}=0.4$ when $\phi\chi_{AB}N=40$ ($\phi=0.2963$, $\chi_{AB}=0.45$ and $N=300$).

We examine the effects of ϕ, χ_{AB}, and N on the distribution of each component when a neutral solvent is added. Fig. 4 demonstrates the deviation of volume fraction profiles ($\phi_I(x)-\bar{\phi}_I$) of component A, B, and S at $y/L=z/L=0.5$ for a series of ϕ at $\chi_{AB}N=41.4$ ($\chi_{AB}=0.138$ and $N=300$). As expected, the addition of more neutral and good solvents into block copolymers reduces the segregation between A and B, resulting in the A and B profiles become more cosine-like. Though the solvent is neutral, it distributes non-uniformally through the segregated domains. In addition to the solvent accumulation behavior at the interfaces, we also observe that the solvent distributes more in the A-rich (minority component-rich) domains than in the B-rich (majority-rich) domains. With decreasing ϕ the solvent profile deviates more from the average solvent volume fraction ($1-\phi$). In Fig. 5 we also plot the deviation profiles for a series of ϕ but $\chi_{AB}N$ increases to 135 ($\chi_{AB}=0.45$ and $N=300$). By comparing the solvent deviation profiles at the same value of the effective $\phi\chi_{AB}N$ but different $\chi_{AB}N$ values in Figs. 4 and 5, we find that even when the effective AB interaction parameter $\phi\chi_{AB}N$ is fixed, the solvent non-uniformity behavior becomes more significant with increasing $\chi_{AB}N$ (i.e. decreasing ϕ). Furthermore, even though both $\chi_{AB}N$ and ϕ are fixed, the distribution of each component is influenced by degree of copolymerization N. This is shown in Fig. 6 where we plot the deviation profiles of each component for a series of N values when $\chi_{AB}N=135$ and $\phi=0.21$. In particular, as N decreases, the non-uniformity degree of solvent distribution through the domains increases.

Varying each parameter ϕ, χ_{AB}, and N hold great influence not only on the distribution of each component but also on the micro-structural length scales. Fig. 7(a)–(d) shows the variation in domain spacing L^*, spherical diameter D^*, interfacial width w^* and matrix length $\Lambda^*(=L^*-D^*-w^*)$ with changes in $\phi\chi_{AB}N$ for a series of ϕ, χ_{AB}, and N values. In Fig. 7 we also present the results for copolymer melts (shown as the solid curve a) as a comparison. At a fixed value of $\chi_{AB}N$ equal to 41.4, when the volume fraction of the added solvent ($1-\phi$) is less than 0.34 so that the solutions are in the same effective segregation regime as the melts, i.e. $27.6\leq(\chi_{AB})_{eff}N=\phi\chi_{AB}N\leq41.4$, the micro-structural length results (shown as the dotted curves b–d) are almost independent of N and the same as those predicted by the dilution approximation, i.e. simply from the melts with $(\chi_{AB})_{eff}=\phi\chi_{AB}$. As $\chi_{AB}N$ increases to 135, the length results (shown as the dashed curves f–i) for the solutions in the same segregation regime (i.e. $1-\phi$ between 0.693 and 0.797) are deviated from the dilution approximation results and strongly dependent on N.

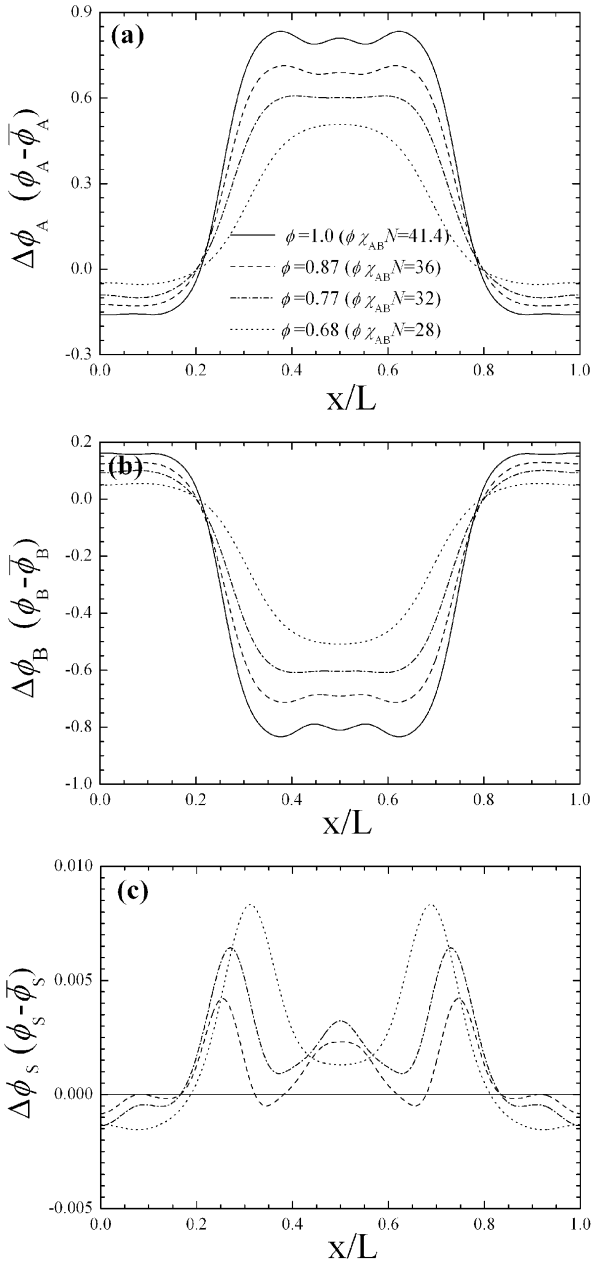

Fig. 4. Deviation of volume fraction profiles $(\phi_I(x) - \bar{\phi}_I)$ for component I = (a) A, (b) B, and (c) S at $y/L = z/L = 0.5$ of a copolymer solution with f = 0.16, $\chi_{AB} = \chi_{BS} = 0.4$, and $\chi_{AB}N = 41.4$ ($\chi_{AB} = 0.138$ and $N = 300$) at a series of ϕ.

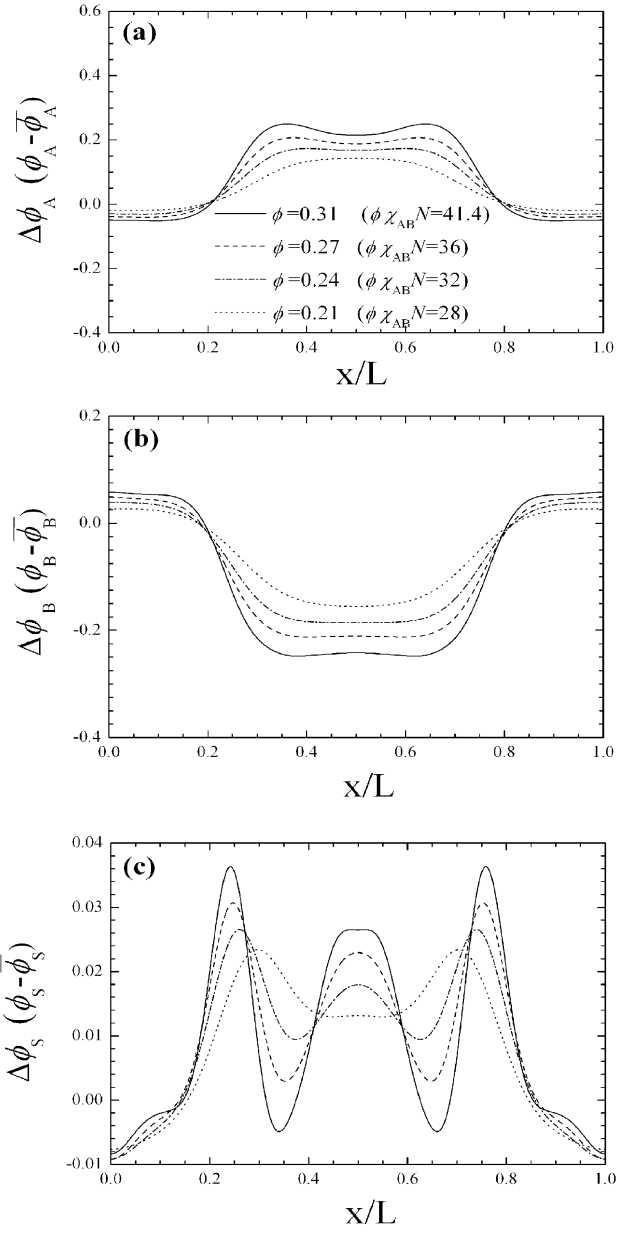

Fig. 5. Deviation of volume fraction profiles $(\phi_I(x) - \bar{\phi}_I)$ for component I = (a) A, (b) B, and (c) S at $y/L = z/L = 0.5$ of a copolymer solution with f = 0.16, $\chi_{AS} = \chi_{BS} = 0.4$, and $\chi_{AB}N = 135$ ($\chi_{AB} = 0.45$ and $N = 300$) at a series of ϕ.

In particular, the length parameters L^*, D^*, Λ^* are significantly smaller than those predicted by the dilution approximation while the interfacial width w^* is larger. The deviation from the copolymer melts increases with decreasing N (i.e. increasing χ_{AB}). We list some typical deviation values for the length parameters L^*, D^*, w^* and Λ^* with respect to those obtained from the melts in Table 1. For example, when $\chi_{AB}N$ is 41.4, the deviations are small to within 4%. As $\chi_{AB}N$ increases to 135, though the deviations for L^* and D^* are within 5%, the deviations for w^* and Λ^* rise significantly up to 9 and 18%, respectively, when N is 300. Fig. 7 also presents the variation of the length results with χ_{AB} for $\phi = 0.7$ and $N = 150$ (shown as curve e), and $\phi = 0.3$ and $N = 150$ (curve j), respectively. It is clear that the deviation increases with decreasing ϕ (i.e. increasing the amount of solvent).

In general, the degree of solvent non-uniformity correlates well with the deviation of structural lengths from the dilution approximation. Furthermore, it is worth noting that this solvent non-uniformity phenomenon has a great influence on the Λ^* including L^* behavior near the ODT, such that the dependence of L^* and Λ^* with respect to $(\chi_{AB})_{eff}N = \phi\chi_{AB}N$ is different from that in melts and varies

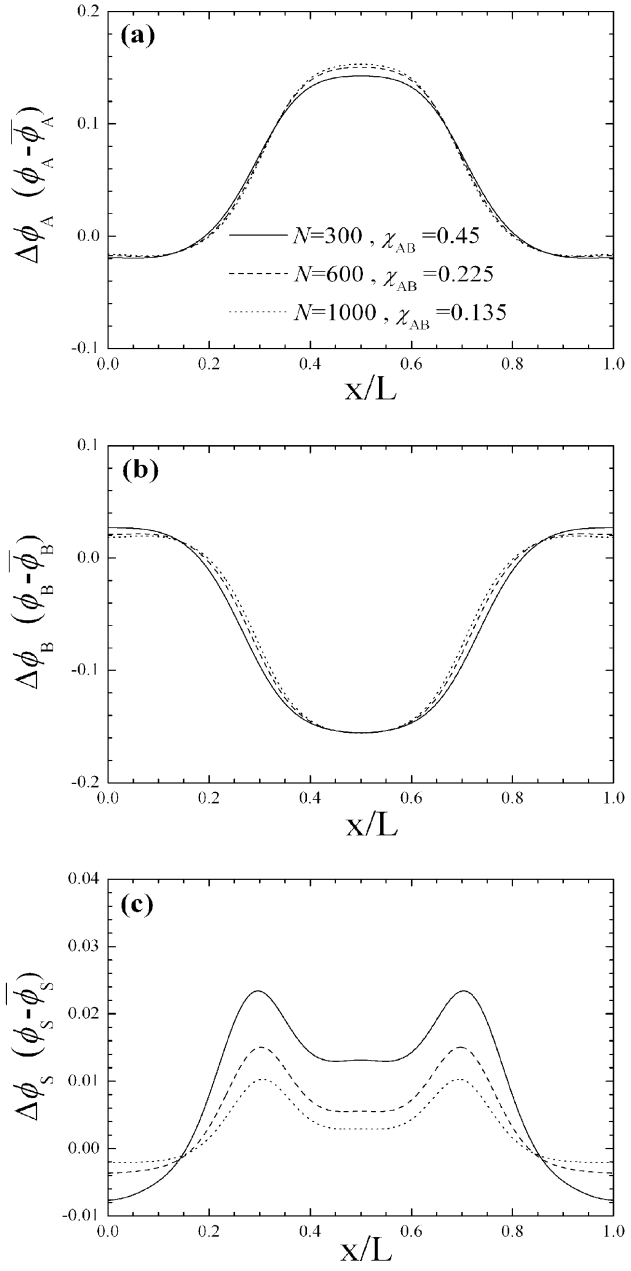

Fig. 6. Deviation of volume fraction profiles ($\phi_I(x) - \bar{\phi}_I$) for component I = (a) A, (b) B, and (c) S at $y/L = z/L = 0.5$ of a copolymer solution with $f = 0.16$, $\phi = 0.207$, $\chi_{AS} = \chi_{BS} = 0.4$, and $\chi_{AB}N = 135$ at a series of N.

with ϕ, χ_{AB}, and N. If we were to express this difference as a power law over the short range of $\phi\chi_{AB}N$ near the ODT, we would find that $L^* \sim (\phi\chi_{AB}N)^{\alpha}$ with the power α varying from -0.45 to -0.05 and $\Lambda^* \sim (\phi\chi_{AB}N)^{\beta}$ with β from -1.98 to -0.5 dependent of ϕ, χ_{AB}, and N. In order to explain this striking behavior, we plot $\tilde{\phi}_J^{(S)}$, $\tilde{\phi}_J^{(W)}$, and $\tilde{\phi}_J^{(M)}$ (J = A, B, S), which correspond to the volume fraction of component J into spheres, interface, and matrix, respectively, for melts and solutions as a function of $\phi\chi_{AB}N$ at a series of χ_{AB} and N in Fig. 8. Recall that for block copolymers in the melt as χ_{AB} decreases because the segregation degree between A and B becomes smaller, the interfacial width w^* increases and both D^* and Λ^* which are characteristic of A-rich and B-rich domains respectively decrease, as expected. As a result L^* decreases with decreasing $\chi_{AB}N$ and scales as $(\chi_{AB}N)^{0.24}$. However, as $\chi_{AB}N$ decreases further and approaches the ODT value, both Λ^* and L^* increase significantly. This is mainly attributed to the fact that many of the minority A blocks are pulled from the spherical domains and swell the matrix, as can be clearly seen in Fig. 8. For a melt with $\chi_{AB}N$ decreasing from 40 to 28 near the ODT, we find that the fraction of A in the interfaces $\tilde{\phi}_A^{(W)}$ decreases slightly from 0.5 to 0.42, and thus a significant increase of A fraction into the matrix $\tilde{\phi}_A^{(M)}$ from 0.2 to 0.52 is mainly attributed to the fraction of A inside the spherical domains $\tilde{\phi}_A^{(S)}$ pulled from 0.3 to 0.06. For component B, though both $\tilde{\phi}_B^{(S)}$ and $\tilde{\phi}_B^{(W)}$ exhibit an increasing and then decreasing behavior, and $\tilde{\phi}_B^{(M)}$ an opposite behavior with decreasing $\chi_{AB}N$, there is not much variation of B fraction in each domain. Thus the sharp increase behavior of L^* and Λ^* near the ODT is consistent with the significant increase of minority A in the matrix domains pulled from the spherical domains. With the addition of a neutral solvent, provided that the solvent amount is not large (for example, $(1-\phi)$ is less than 0.34 when $\chi_{AB}N = 41.4$), the factions of A and B components into each regime are the same as those for melts, and the solvent fractions into each regime behave similar to the A fractions. Therefore, the dependence of L^*, D^*, Λ^*, and w^* with ϕ near the ODT behaves much the same as that with respect to $\chi_{AB}N$ for a melt. As the added solvent amount and/or $\chi_{AB}N$ continues increasing (for example, when $\chi_{AB}N = 138$ such that $1-\phi$ is around 0.71–0.80), we find that the fractions of each component into spheres are almost the same, but those into interfaces increase and those into matrix regimes decrease with the values for melts and for concentrated solutions. As such, the increase of the degree for the minority blocks pulled from the spheres into the matrix near the ODT is not as significant as that in the melt. The sharp increase behavior in L^* as well as Λ^* near the ODT gets smoothened and even disappears.

It should be noted that all of the above results are based on the self-consistent mean-field theory. It is well known that near the ODT in the semidilute regime the effects of chain swelling as well as the fluctuations have to be considered. If so, these effects may influence the domain size in two opposite ways. On the one hand, the swelling chains will lead to larger domain spacing, as one may naively expect. On the other hand, if the neutral solvent accumulates at the A/B interfaces, the area per chain increases which thus leads to a decrease of the domain spacing. We believe that this solvent accumulation behavior becomes more significant with the fluctuation effects considered. Therefore, it is reasonable to expect that the domain spacing becomes smaller than the mean-field prediction. As such, the deviation from the dilution approximation becomes larger and our results near the ODT become more significant.

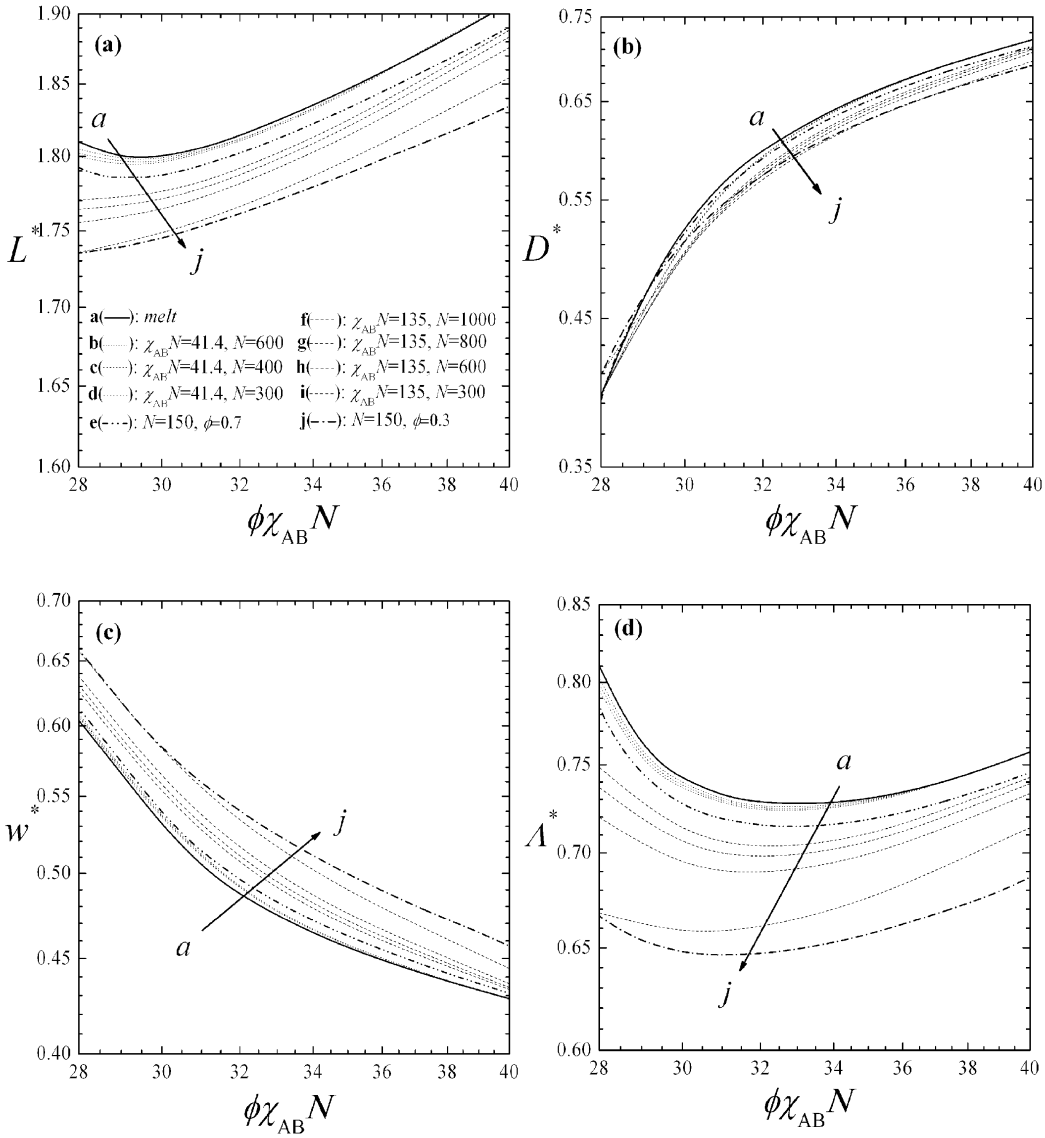

Fig. 7. Double-logarithmic plot of (a) lattice spacing L^*, (b) spherical diameter D^*, (c) interfacial width w^*, and (d) matrix domain length Λ^* versus $\phi\chi_{AB}N$ at various values of χ_{AB} and N for block copolymer solutions with $f=0.16$ and $\chi_{AS}=\chi_{BS}=0.4$ in the S_A^{BCC} phase.

Table 1
Typical values of deviation for the length parameters L^*, D^*, w^* and Λ^* compared with those obtained from the melts

$\chi_{AB}N$	χ_{AB}	N	$\phi\chi_{AB}N$	(%)			
				$(L^*(\phi=1)-L^*(\phi))/(L^*(\phi=1))$	$(D^*(\phi=1)-D^*(\phi))/(D^*(\phi=1))$	$(w^*(\phi)-w^*(\phi=1))/(w^*(\phi=1))$	$(\Lambda^*(\phi=1)-\Lambda^*(\phi))/(\Lambda^*(\phi=1))$
41.4	0.207	200	28	1.239	0.423	0.846	3.192
			36	0.133	0.250	0.309	0.295
	0.069	600	28	0.283	0.042	0.386	0.941
			36	0.022	0.072	0.178	0.099
135	0.450	300	28	4.115	3.493	8.960	17.573
			36	2.785	3.582	3.776	3.776
	0.135	1000	28	2.179	0.042	3.691	7.648
			36	1.015	1.296	1.128	1.961

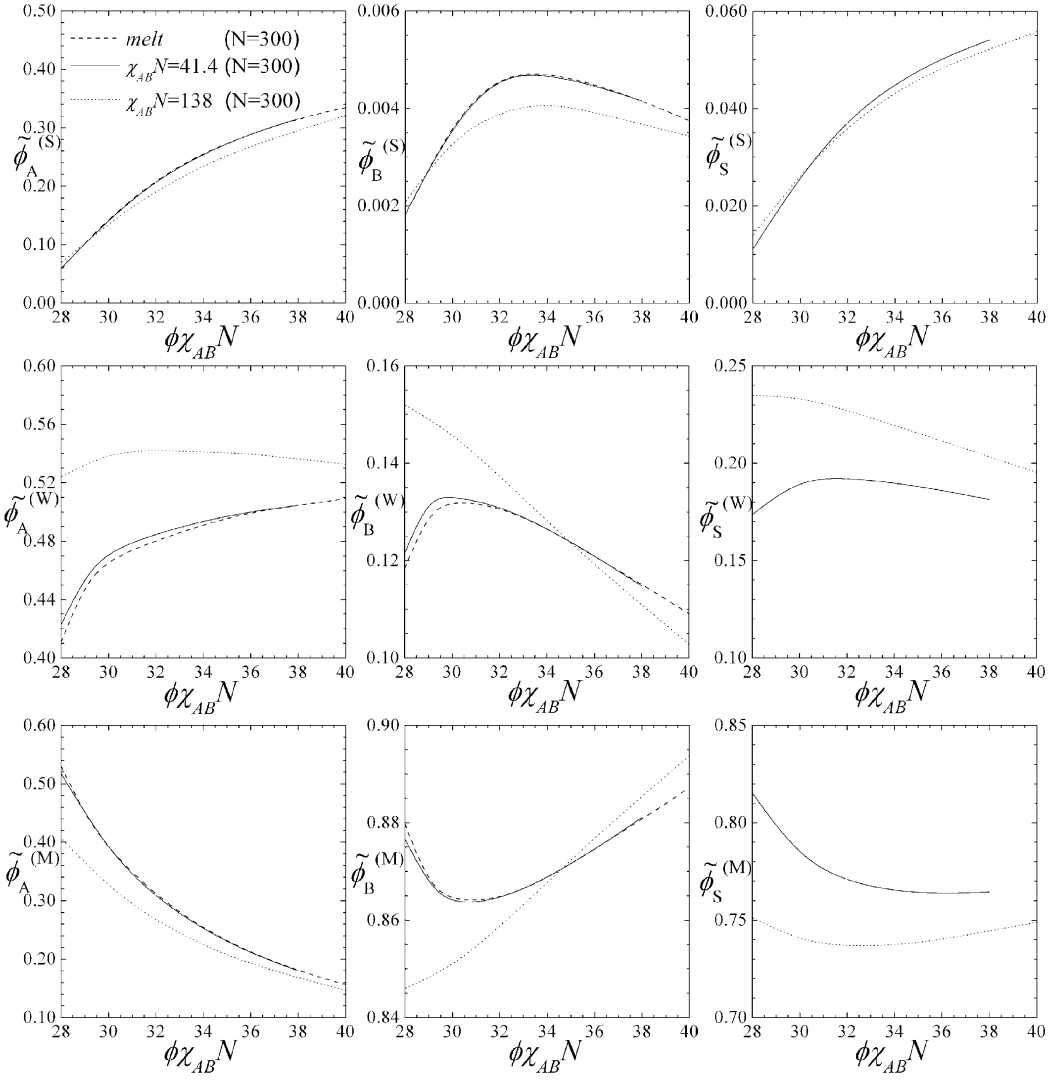

Fig. 8. Volume fraction of component J (J = A, B, S) into the spheres, interface, and the matrix, $\phi_J^{(S)}$, $\phi_J^{(W)}$, and $\phi_J^{(M)}$, respectively, for melts and solutions as a function of $\phi\chi_{AB}N$ at various values of χ_{AB} and N for block copolymer solutions with $f=0.16$ and $\chi_{AS}=\chi_{BS}=0.4$ in the S_A^{BCC} phase.

4. Conclusions

In this paper we analyze the distribution behavior of each component as well as the micro-structural length scales for the body-centered cubic (bcc) spheres of A/B diblock copolymers in a neutral solvent by self-consistent mean-field (SCMF) theory calculations. In particular, the effects of χ_{AB}, N, and ϕ are examined. Most previous theoretical studies have shown that with the dilution of a neutral and good solvent into block copolymers, the domain spacing L^* is simply obtained as a neat copolymer with the effective A/B interaction parameter $(\chi_{AB})_{eff}=\phi\chi_{AB}$, i.e. L^* obeys the so-called dilution approximation. While our SCMF results for the bcc phase find that the length parameters become more complicated due to the effects of solvent non-uniformity and are strongly dependent of each parameter χ_{AB}, N, and ϕ. With increasing solvent amount $(1-\phi)$ and/or $\chi_{AB}N$, the domain spacing L^*, the spherical diameter D^*, and the matrix length Λ^* are significantly smaller than those predicted by the dilution approximation while the interfacial width w^* is larger. Although when $\chi_{AB}N$ is fixed, the deviation increases with decreasing N. In general, the deviation of micro-structural lengths from the dilution approximation correlates well with the degree of solvent non-uniformity.

Furthermore, when ODT is approached, both the dependence of L^* and Λ^* with respect to $(\chi_{AB})_{eff}N=\phi\chi_{AB}N$ for the solutions exhibit a strikingly different behavior with that for melts. Recall that for melts in the bcc spheres L^* and Λ^* both increase sharply as the ODT is approached. This sharp increase of behavior near the ODT, in particular for copolymers with a very short minority block, is not surprising due to the fact that many of the minority blocks are pulled from the spherical domains and thus swell the matrix. With increasing solvent amount and/or $\chi_{AB}N$, the fractions of each component into

interfaces increase and those into matrix regimes decrease with those values for melts as well as for concentrated solutions. As such, the increase of the degree for the minority blocks pulled from the spheres into the matrix near the ODT is not as significant as that in the melt. The sharp increase in the behavior of L^* as well as Λ^* near the ODT smoothens and even disappears. If we were to express this difference as a power law over the short range of $\phi\chi_{AB}N$ near the ODT, we would find that L^*(in terms of $\sqrt{N}b$) $\sim (\phi\chi_{AB}N)^{\alpha}$ with the power α varying from -0.45 to -0.05 and $\Lambda^* \sim (\phi\chi_{AB}N)^{\beta}$ with β from -1.98 to -0.5 dependent of ϕ, χ_{AB}, and N. It should be noted that this unique behavior for L^* and Λ^* near the ODT in the bcc phase due to the effects of solvent addition has not been observed elsewhere.

Acknowledgements

This work was supported by the National Science Council of the Republic of China through grant NSC 92-2216-E-002-033. We are grateful to Dr An-Chang Shi for helpful discussions.

References

[1] Lodge TP. Macromol Chem Phys 2003;204:265.
[2] Hadjichristidis N, Pispas S, Floudas CA. Block copolymers. New Jersey: Wiley; 2003.
[3] Förster S, Plantenberg T. Angew Chem, Int Ed 2002;41:688. Förster S, Antonietti M. Adv Mater 1998;10:195.
[4] Helfand E, Tagami Y. J Chem Phys 1972;56:3592.
[5] Hong KM, Noolandi J. Macromolecules 1983;16:1083.
[6] Fredrickson GH, Leibler L. Macromolecules 1989;22:1238.
[7] Olvera de la Cruz M. J Chem Phys 1989;90:1995.
[8] Whitmore MD, Noolandi J. J Chem Phys 1990;93:2946.
[9] Whitmore MD, Vavasour JD. Macromolecules 1992;25:2041.
[10] Vavasour JD, Whitmore MD. Macromolecules 1992;25:5477.
[11] Huang CI, Lodge TP. Macromolecules 1998;31:3556.
[12] Vavasour JD, Whitmore MD. Macromolecules 2001;34:3471.
[13] Naughton JR, Matsen MW. Macromolecules 2002;35:5688.
[14] Hashimoto T, Shibayama M, Kawai H. Macromolecules 1983;16:1093.
[15] Shibayama M, Hashimoto T, Hasegawa H, Kawai H. Macromolecules 1983;16:1427.
[16] Hashimoto T, Mori K. Macromolecules 1990;23:5347.
[17] Lodge TP, Pan C, Jin X, Liu Z, Zhao J, Maurer WW, Bates FS. J Polym Sci, Polym Phys 1995;33:2289.
[18] Mori K, Atsuo O, Hashimoto T. J Chem Phys 1996;104:7765.
[19] Sakurai S, Hashimoto T, Fetters LJ. Macromolecules 1996;29:740.
[20] Sakamoto N, Hashimoto T, Han CD, Kim D, Vaidya NY. Macromolecules 1997;30:5321.
[21] Lodge TP, Hamersky MW, Hanley KJ, Huang CI. Macromolecules 1997;30:6139.
[22] Huang CI, Chapman BR, Lodge TP, Balsara NP. Macromolecules 1998;31:9384.
[23] Hanley KJ, Lodge TP. J Polym Sci, Polym Phys 1998;36:3101.
[24] Hanley KJ, Lodge TP, Huang CI. Macromolecules 2000;33:5918.
[25] Lodge TP, Hanley KJ, Pudil B, Alahapperuma V. Macromolecules 2003;36:816.
[26] Matsen MW, Bates FS. J Chem Phys 1997;106:2436.